

Article

The Investigation of High Quality PEDOT:PSS Film by Multilayer-Processing and Acid Treatment

Po-Wen Sze ¹, Kuan-Wei Lee ², Pin-Chiao Huang ³, Dei-Wei Chou ⁴, Bing-Siang Kao ⁵
and Chien-Jung Huang ^{5,*}

¹ Department of Electrical Engineering, Kao-Yuan University, Kaohsiung 821, Taiwan; t20029@cc.kyu.edu.tw

² Department of Electronic Engineering, I-Shou University, Kaohsiung 84008, Taiwan; kwlee@isu.edu.tw

³ Department of Electrical Engineering, National Chung Hsing University, Taichung 40227, Taiwan; diamondjubileeya@gmail.com

⁴ Department of Aviation & Communication Electronics, Air Force Institute of Technology, Kaohsiung 820, Taiwan; cdvwp0801@yahoo.com.tw

⁵ Department of Applied Physics, National University of Kaohsiung, Kaohsiung 81148, Taiwan; m1034301@mail.nuk.edu.tw

* Correspondence: chien@nuk.edu.tw; Tel.: +886-7-591-9475; Fax: +886-7-591-9357

Academic Editor: Jean-Michel Nunzi

Received: 29 March 2017; Accepted: 15 May 2017; Published: 18 May 2017

Abstract: In this study, we have investigated the performance of multilayer films of poly(3,4-ethylenedioxythiophene):poly(styrenesulfonate) (PEDOT:PSS) treated with one of the perfluorinated carboxylic acids, named trifluoroacetic acid (TFA). According to the increased density of the PEDOT chain under unit area conditions, the sheet resistance (R_{sq}) has improved from 300 to 65 Ω /sq through additional processing of PEDOT:PSS from single layer to multilayer. After the further treatment with TFA, however, the R_{sq} of the multilayer PEDOT:PSS was enhanced to 45 Ω /sq, leading to the decline of film thickness from 400 to 270 nm. Both conductivity and work function based on X-ray photoelectron spectroscopy results have built a breakthrough by double-processing because of the higher density of conductive PEDOT chains and the increase of 0.4 eV alternatives to typical indium tin oxide substrate, respectively. This improvement is contributed to the development of more effective transparent electrodes.

Keywords: double processing; organic solar cells; transparent electrode; sheet resistance

1. Introduction

In recent years, flexible optoelectronic devices such as organic light-emitting diodes, organic solar cells, perovskite solar cells, touch panel displays, and electronic paper have drawn considerable research attention. Developments in these fields are particularly important for next generation displays, which may offer optoelectronic devices fabricated by low cost roll-to-roll process that are lightweight and mechanically flexible [1,2]. Indium tin oxide (ITO) has been widely used as a transparent electrode in optoelectronic devices. However, ITO has several drawbacks, including its high brittleness, which makes it unsuitable for flexible electronic devices. Furthermore, the scarcity of indium and high demand for its compounds has resulted in the increase of its cost. The ITO components of polymer solar cells comprise a large portion of their overall cost [3]. Additionally, ITO has some inherent problems such as poor transparency on short wavelengths of visible light (400 to 500 nm), a need for high temperature processing, and the potential for oxygen and indium to diffuse into the organic layer [4]. To address these problems, academia and industry are actively investigating new transparent conductive materials to replace ITO.

Many materials have been investigated as transparent electrodes; however, poly(3,4-ethylenedioxythiophene):poly(styrenesulfonate) (PEDOT:PSS) is considered to be one of the best transparent conductor candidates. PEDOT:PSS is a conductive composite of two polymers (PEDOT and PSS). PEDOT is insoluble in water and based on the 3,4-ethylenedioxythiophene (EDOT) monomer unit. PEDOT can form an aqueous suspension when combined with PSS, improving its process ability. PEDOT:PSS is superior to other materials because of its workability, mechanical flexibility, and optical properties [5]. Despite these advantages, the low conductivity of PEDOT:PSS restricts its application in optoelectronic devices [6–11]. However, the carrier transport (buffer) layer of anode and cathode has played an important role for solar cells, such as Metal oxide material (MoO_3 , WO_3) and PEDOT:PSS. Therefore, many researchers have studied ways to enhance the conductivity of PEDOT:PSS. Several techniques have been proposed to increase the conductivity of PEDOT:PSS films by adding organic compounds, such as sorbitol [12–15], dimethyl sulfoxide (DMSO) [15–18], glycerol [15,19,20], ethylene glycol (EG) [21–23], polyethylene glycol, and boric acid [22–24]. Nevertheless, the conductivity of such modified PEDOT:PSS films remains very low for practical applications. In this study, the conductivity of PEDOT:PSS is considerably enhanced by forming multilayered PEDOT:PSS films and using an organic acid treatment. The mechanism by which the PEDOT:PSS film conductivity was optimized is also studied.

2. Experimental Methods

The ITO glass substrate is obtained by a commercial source with $7 \Omega/\text{sq}$ to become the basis for comparison. The PEDOT:PSS (Clevios PH 1000, Uni-onward corp., Taipei, Taiwan) doped with sorbitol (98%, Uni-onward corp., Taipei, Taiwan) was used as the solution for the preparation of the stacked multilayer film. Glass substrates with an area of $1.5 \times 1.5 \text{ cm}^2$ were pre-cleaned with acetone, methanol, and deionized water (DI) water in an ultrasonic for 10 min each time, sequentially. The cleaned glass substrates were treated with UV/ozone for 60 s prior to spin coating. The PEDOT:PSS solution, which filtered through a syringe filter (0.45 mm pore size), was spin-coated on the clean glass substrate. The spin-coating was performed at a different rotation rate for 30 s. The PEDOT:PSS film was heated at $150 \text{ }^\circ\text{C}$ for 20 min on a hot plate in ambient conditions. Afterward, thicker PEDOT:PSS films were prepared by spin coating multiple times, and annealing and film treatment was done after each layer.

In addition, the acid treatment was carried out by dropping an acid solution of $100 \mu\text{L}$ on a PEDOT:PSS film. The PEDOT:PSS film is slightly rinsed by immersion in the DI water. Trifluoroacetic acid (TFA, Uni-onward corp., Taipei, Taiwan) is an organofluorine compound with the chemical formula $\text{CF}_3\text{CO}_2\text{H}$. We have researched the effect of TFA on PEDOT:PSS because it is a colorless liquid with a sharp odor similar to vinegar but stronger in acidity. TFA is an analogue of acetic acid with the three hydrogen atoms replaced by three fluorine atoms. The acidity of TFA is approximately 34,000 times stronger than that of acetic acid due to the electronegativity of the trifluoromethyl group. At the same time, TFA is widely used in organic chemistry for various purposes. Subsequently, the PEDOT:PSS film is dried at $150 \text{ }^\circ\text{C}$. The R_{sq} of double treated PEDOT:PSS films were measured with a four-point sheet resistivity meter (SRM103, Solar Energy Tech., Taiwan). The film thickness was measured using alpha step surface profiler (Surfcorder ET400M, Tainan, Taiwan). The X-Ray photoelectron spectroscopy (XPS) was measured by an X-ray photoelectron spectrometer (JEOL, JAMP-9500F, Kaohsiung, Taiwan). The surface morphology and roughness of the PEDOT:PSS films were measured by atomic force microscopy (AFM, Park Systems, XE-70, Suwon, Korea), and the transmittance of the PEDOT:PSS films was measured by a UV/visible spectrometer (UV-3900, Hitachi, Tokyo, Japan). The work function of the PEDOT:PSS films was measured as the surface potential (V_{CPD}) of the films by scanning Kelvin probe microscopy (SKPM, Park Systems, XE-100).

3. Results and Discussion

The PEDOS:PSS shows the chemical molecular structure and general arrangement under solution in Figure 1a. The chains of PEDOT are obviously much shorter than those of PSS, and the combination of both of them is due to the Columbic attraction. It is believed that the conductivity of the thin film of PEDOT:PSS can be enhanced after a series of material processes in Figure 1b,c, including heating and the addition of sorbitol dopant. The sorbitol additive interacts with PEDOT and PSS, causing their chains to separate in solution in Figure 1b. At the same time, this treatment causes the coiled PEDOT and PSS chains to rearrange into linear chains [25–27]. In addition, Figure 1c has shown the schematic of heating PEDOT:PSS with sorbitol. The evaporation of the solution during film baking allows the PEDOT:PSS chains to be much closer in order to rearrange, in comparison to the situation with sorbitol. The rearrangement of PEDOT:PSS leads to the two polymers being closer to each other. This reduces the hopping distance between the PEDOT chains and enhances the conductivity of the PEDOT:PSS film.

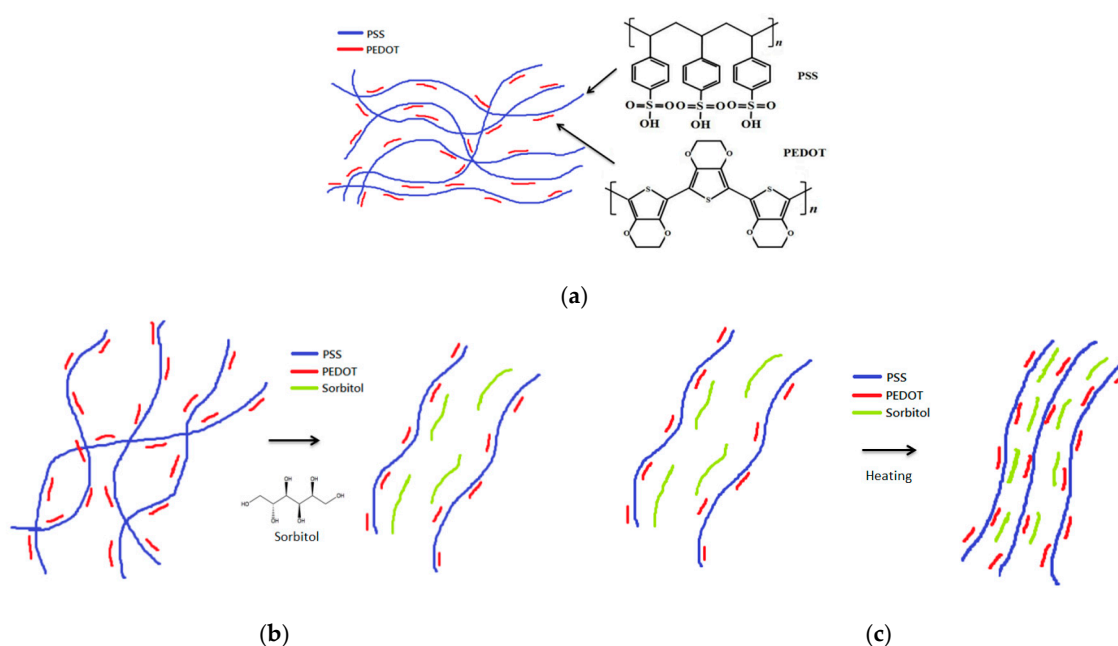


Figure 1. The investigation includes the (a) chemical structure of PEDOT:PSS; (b) the rearrangement of PEDOT:PSS with sorbitol; and (c) the schematic illustration of the heating of PEDOT:PSS with sorbitol.

The effects on transmittance, R_{sq} , and the films' thickness are investigated in detail after spin-coating fabrication. Figure 2 shows the transmittance, R_{sq} , and film thickness of a single PEDOT:PSS layer processed under different spin coating conditions. Transmittance increased at higher spin-coating speeds. It is likely that the distribution of PEDOT:PSS chains with wider sizes is more discretely arranged in the thin film, resulting in higher transmittance. Conversely, the R_{sq} decreased in the films spun at lower spin speeds. This indicates a narrower size distribution of the arranged PEDOT:PSS chains, contributing to lower sheet resistance and film thickness. Notably, the R_{sq} is related to film thickness. However, the conductivity of the single layer PEDOT:PSS film remained very low for practical applications.

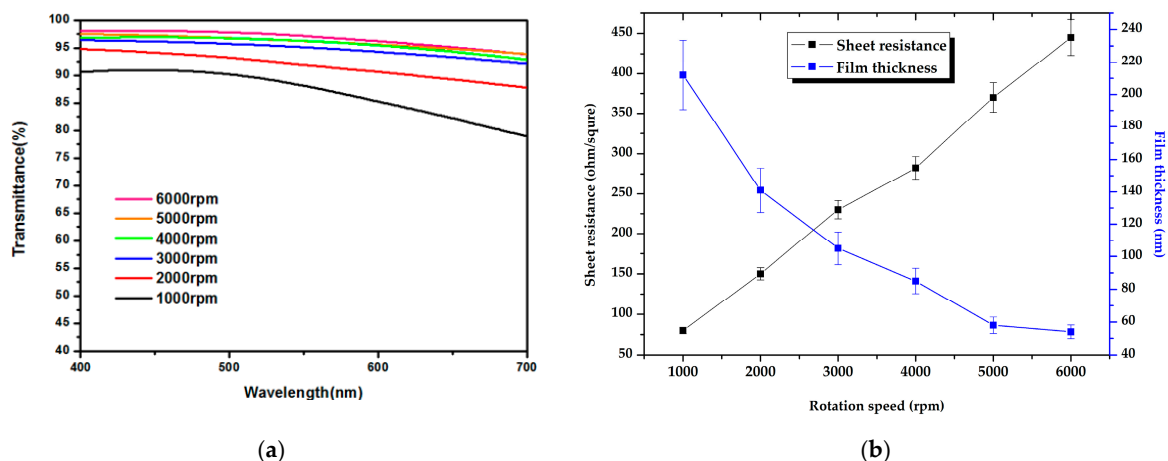


Figure 2. (a) Transmittance and (b) sheet resistance (R_{sq}) and film thickness for PEDOT:PSS of single layer films with different rotational speeds.

The transmittance of the different multilayer PEDOT:PSS film in the visible wavelength is shown in Figure 3a, and the three layers (PEDOT:PSS films) remained of a higher value than typical ITO film from 400 to 500 nm. The transmittance values in the whole visible spectrum of one, three, and five layers of PEDOT:PSS were 97.1%, 90.1%, and 81.1%, respectively. Figure 3b shows the variation of R_{sq} and transmittance with film thickness for the multilayer PEDOT:PSS films. The R_{sq} for the films was 283, 100, and 69 Ω/sq with thicknesses of 86, 250, and 400 nm, respectively, whereas the transmittances were 97%, 90%, and 79%, respectively. The layering process increased the PEDOT chain content per unit area, thus reducing the resistivity of the PEDOT:PSS films. The R_{sq} of a single layer was around 283 Ω/sq but decreased to 100 Ω/sq in the multilayered films. To meet the requirements of a functional electrode, different experimental parameters, including film thickness, R_{sq} , and transmittance, were adjusted, and the results are shown in Table 1. To obtain smoother films, a higher spin-coating speed was used. The first three layers of the PEDOT:PSS films were spin-coated at a rotation rate of 4000 rpm. The other two layers were spun at 6000 rpm to obtain the optimal R_{sq} of PEDOT:PSS films. Additionally, the thickness of processed PEDOT:PSS is increased under the condition of the change of ten counts.

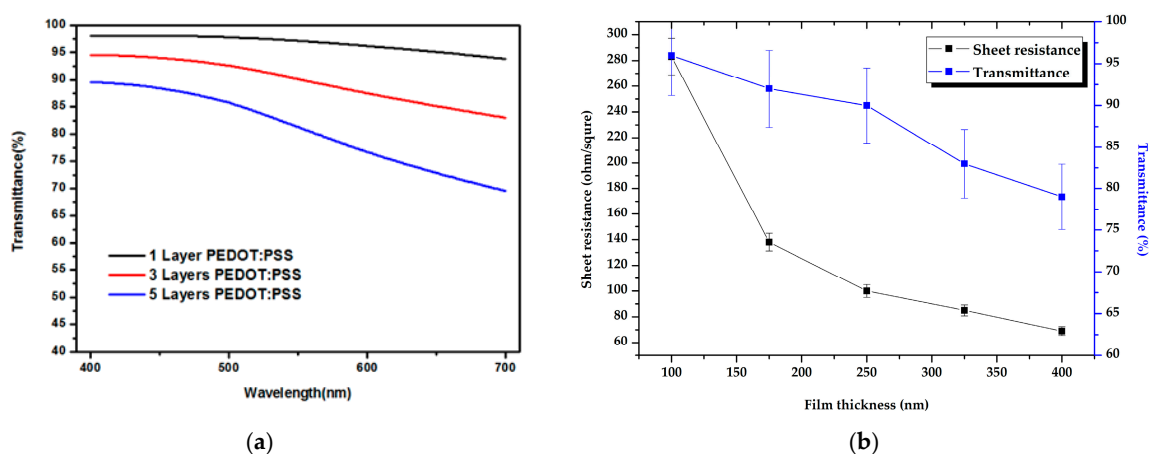


Figure 3. (a) Transmittance of one, three, and five layers of PEDOT:PSS films; (b) Variation of R_{sq} and the transmittance of average value in the visible wavelength with film thickness for PEDOT:PSS.

Table 1. The film thickness (d), sheet resistance (R_{sq}), and transmittance (T) of average value in the visible wavelength for PEDOT:PSS films (PH1000: 4 wt% Sorbitol), which are spin-coated at both 4000 and 6000 rpm, is compared to the result of trifluoroacetic acid (TFA) treatment.

Layer (s)	d (nm)	R_{sq} (Ω/sq)	T (%)
1	86	283	97
3	250	90	90
5	400	69	79
5 with TFA treatment	325	45	82

A schematic of PEDOT:PSS films treated with trifluoroacetic acid (TFA) is shown in Figure 4. After forming the PEDOT:PSS film on a glass substrate, the surface of the film was treated with TFA. The mechanism of conductivity enhancement is related to the H^+ transfer from the acid to the PSS^- groups of PEDOT:PSS. This can be expressed as $CF_3CO_2H + PSS^- \rightarrow C_2F_3O_2^- + PSSH$. $C_2F_3O_2^-$ forms an ionic bond with PEDOT, and the PSS^- groups capture protons, neutralizing their charge. This reduces the Coulombic attraction between the $PEDOT^+$ and PSS^- chains [28]. However, PSS^- can not be completely converted to $PSSH$, and some of the PEDOT chains retain PSS^- chains. The hydrophilic PSS chains can be easily removed from the surface of PEDOT:PSS films by rinsing with deionized water. This lowers the R_{sq} ; first, by increasing the relative proportion of PEDOT chains at the film surface; second, the TFA behaves as a dehydrating agent as the solution vaporizes. Thus, the energy barriers for inter-chain and inter-domain charge hopping are lowered, allowing for better charge transfer along the PEDOT chains.

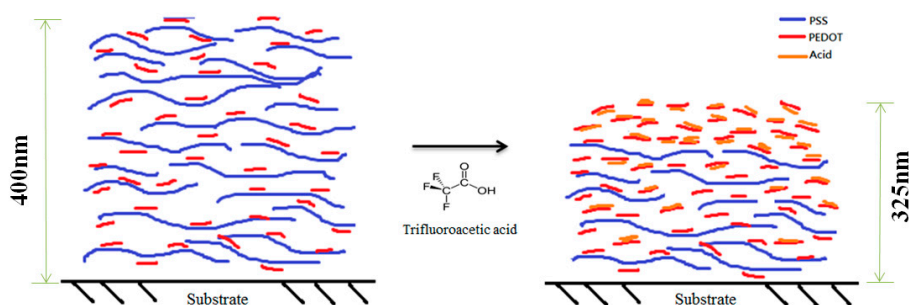


Figure 4. The schematic illustration of the mechanism for conductivity enhancement of PEDOT:PSS films by treatment with organic acid (TFA).

The spin-coating speed, film thickness, R_{sq} , and transmittance values of untreated and acid treated PEDOT:PSS multilayers are shown in Table 1. The R_{sq} of a PEDOT:PSS film as an anode depends on its thickness. The thickness of the acid-treated films was 325 nm, which was lower than that of untreated pristine multilayer films (400 nm). Under the same conditions, the treated film had a R_{sq} of 45 Ω/sq . Since the film thickness decreased, the transmittance of the treated PEDOT:PSS film also slightly increased from 79% to 82%.

The conformational change of the PEDOT chains after the double-processing method was further studied by Raman spectroscopy. Figure 5 shows the Raman spectra of the pristine, the sorbitol added PEDOT:PSS solution, and the TFA treated PEDOT:PSS films. The strongest band of Raman between 1400 and 1500 cm^{-1} corresponds to the stretching vibration of the $C_{\alpha} = C_{\beta}$ bonds of PEDOT chains [29,30]. Furthermore, there are two peaks at the benzenoid vibration of 1440 cm^{-1} and quinoid vibration of 1415 cm^{-1} . The benzenoid structure is the coil conformation. The quinoid structure is the expanded-coil or the linear conformation [29,31]. The peak value shifts from 1440 to 1415 cm^{-1} after the post-treatment, indicating that the resonant structure of the PEDOT chains changes from the benzenoid structure to the quinoid structure.

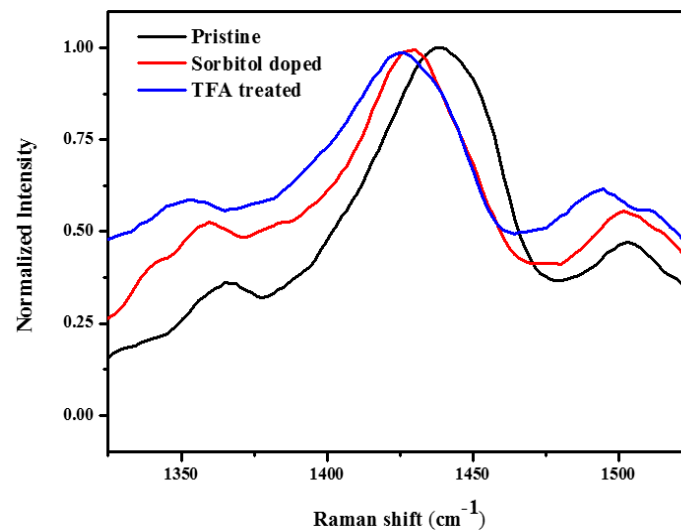


Figure 5. The Raman spectra of the pristine, the Sorbitol added PEDOT: PSS solution, and the TFA treated PEDOT:PSS films.

Figure 6a shows the X-ray photoelectron spectroscopy (XPS) of single layer and multilayer PEDOT:PSS films. The XPS signal peaks between 162 and 166 eV correspond to the sulfur atom of PEDOT [32–34]. The signal near 169 eV corresponds to the sulfur atom of PSS. The PEDOT:PSS ratio was calculated from the areas under each peak using integral calculus. The PEDOT:PSS ratio increased from 0.355 before film treatment to 0.422 after film treatment. Figure 6b shows the XPS spectra of PEDOT:PSS multilayer films before and after acid treatment. The ratio increased further to 0.588 after dropping TFA on the film. However, the PEDOT:PSS ratio of the surface region of the multilayer films increased to a value 56% greater than that of the single layer film. Increasing the PEDOT-rich chains was expected to enhance the conductivity of the PEDOT:PSS film by forming better connecting pathways with other PEDOT chains.

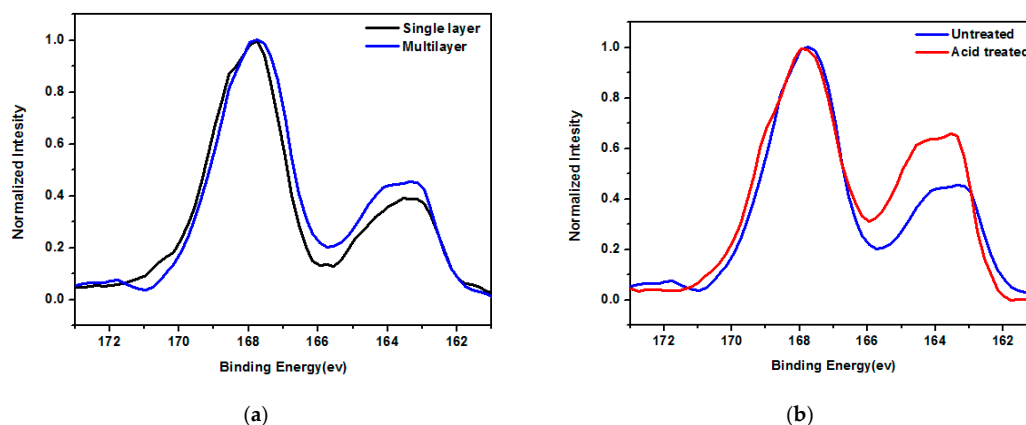


Figure 6. The S (2p) XPS spectra of (a) single layer and multilayer film and (b) untreated and acid treated film.

Figure 7 shows that the film morphology changed after the multilayer and TFA treatments. In the AFM images, the bright and dark phase regions correspond to the PEDOT and PSS grains, respectively [35–37]. The roughness of a single layer of untreated PEDOT:PSS was 1.141 nm. The phase image is homogeneous, indicating weak phase separation between PEDOT and PSS and low surface roughness. The roughness of the untreated multilayer PEDOT:PSS film with five layers was higher than that of the single layer at 1.873 nm. After TFA treatment of the same PEDOT:PSS film, the surface

roughness increased to 2.795 nm. The decreased R_{sq} measured for the multilayer PEDOT:PSS film subjected to both multilayer and acid treatments is consistent with our previous findings. These findings suggested that the polymer nanoparticles swell and aggregate together after the TFA treatment of the PEDOT:PSS films. However, the connectivity of the PEDOT:PSS film is improved between conductive regions, with the result that the compact and fiber-like PEDOT-rich chains facilitate charge transport. Incidentally, the surface roughness of the TFA-treated film remained considerably lower than that of a typical ITO substrate (4.961 nm).

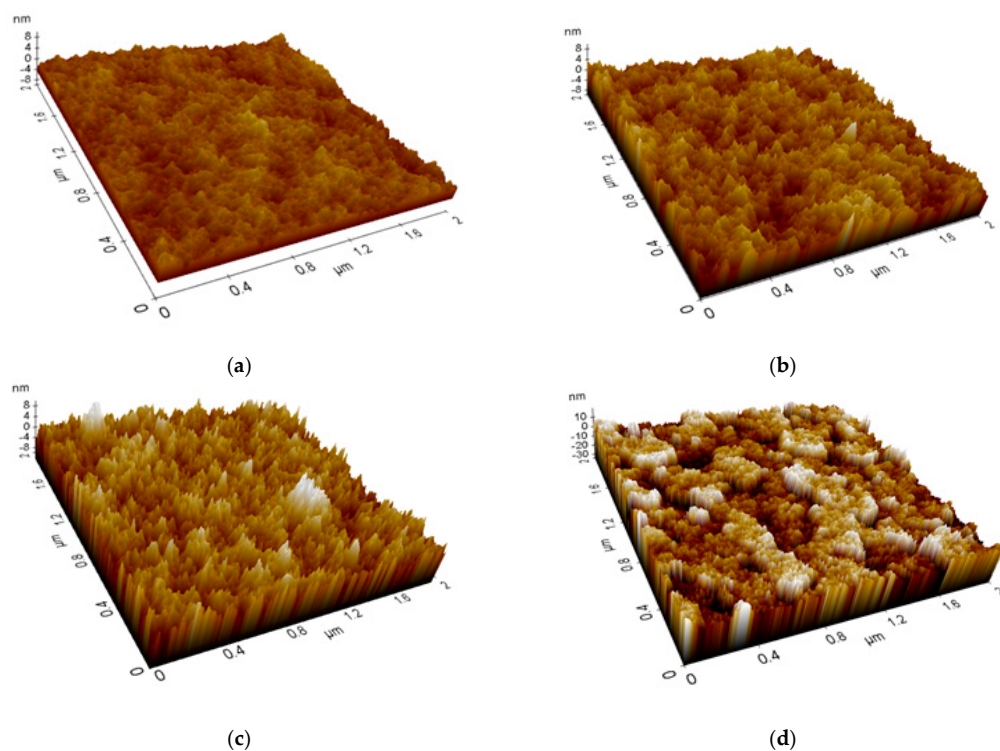


Figure 7. The atomic force microscopy (AFM) images of (a) single layer PEDOT:PSS films; (b) multilayer PEDOT:PSS films; (c) multilayer PEDOT:PSS films treated with organic acid; and (d) Indium tin oxide (ITO).

PEDOT:PSS is the most widely used anode material that has a high work function, ensuring its effectiveness in transporting holes to the anode [38]. The work functions of PEDOT:PSS films fabricated by different processes are shown in Table 2. These include films with sorbitol additives and multilayer and acid-treated films. To determine the work function of acid-treated multilayer PEDOT:PSS films, we measured the surface potential (V_{CPD}) by scanning Kelvin probe microscopy. The surface potential relates to the work function as $V_{CPD} = (\Phi_{tip} - \Phi_{sample})/q$, where Φ_{tip} and Φ_{sample} are the work functions of the tip and sample, respectively [39]. Taking 4.6 eV as the work function of highly oriented pyrolytic graphite (HOPG) was typically used as reference of SKPM measurement [40]. The measured work functions of the acid-treated multilayer PEDOT:PSS thin films ranged from 4.8 to 5.1 eV, compared with 4.7 eV for ITO.

Table 2. Work function of PEDOT:PSS films spin cast with different processes.

Process	Work Function (eV)
PEDOT:PSS films with sorbitol	4.87
Multilayer of PEDOT:PSS films	5.08
Acid-treated PEDOT:PSS films	5.12
Typical ITO sample	4.78

Figure 8 shows the sign of the work function change for double-processing methods. In the situation without this dipole layer (Figure 8a), the work function is explained in the sorbitol added to the PEDOT: PSS films [13,41]. The shift Δ in work function is consistent with the rich surface layer that is present in PEDOT: PSS films. In Figure 8b,c, the increased the work function leads to the fact that the PSS-rich and TFA ion-rich top layers result in an inward directed surface potential dipole. The variation of the work function is related to the magnitude of the shift Δ depending on the surface layer thickness. Therefore, upon an increase of the surface layer thickness by double-processing methods, the work function will be enhanced.

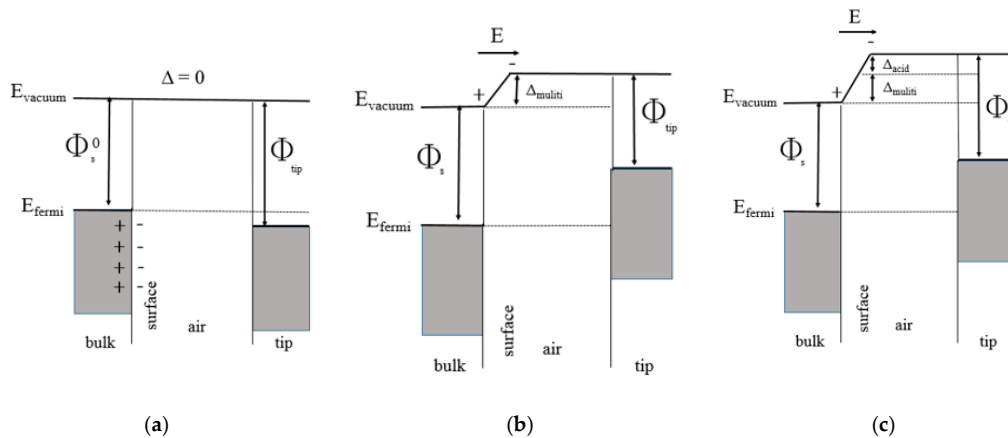


Figure 8. Schematic representation of the band diagrams during scanning Kelvin probe microscopy (SKPM) on PEDOT:PSS thin films. (a) sorbitol-treated PEDOT:PSS without PSS surface layer; (b) multilayer PEDOT:PSS with a PSS-rich surface layer; and (c) acid-treated PEDOT:PSS with a TFA ion-rich surface layer. ϕ_s^0 , ϕ_s and ϕ_{tips} , are, respectively, the work functions of sorbitol-treated PEDOT:PSS thin film, multilayer “bulk” PEDOT:PSS, and the tip. Δ_{multi} and Δ_{acid} are the surface dipole due to the PSS-rich and TFA ion-rich surface layer, which effectively enhances the film work function to $\phi_s + \Delta_{multi}$ and $\phi_s + \Delta_{multi} + \Delta_{acid}$, respectively.

4. Conclusions

We have fabricated the acid-treated multilayer PEDOT:PSS films exhibiting low R_{sq} and transmittance. It is found that the R_{sq} is enhanced from 283 to 69 Ω/sq in films comprising multiple PEDOT:PSS layers. Additionally, the R_{sq} of stacked PEDOT:PSS increases to 45 Ω/sq after treatment with TFA. The transmittance of the PEDOT:PSS films subjected to both treatments was 82% in the visible wavelength range from 400 to 700 nm. The measured work function of the treated PEDOT:PSS thin film is 5.1 eV compared with 4.7 eV for a typical ITO sample. The mechanism of conductivity enhancement of the PEDOT:PSS film is investigated. There is a model for optimal PEDOT:PSS film processing. Based on this model, we have determined four important factors for improving the quality of PEDOT:PSS films: phase separation between PEDOT and PSS; increasing film thickness; enhancing PEDOT chain content per unit area; and the application of an organic acid treatment. Various techniques, including physical, chemical, and electrical characterizations, have showed that acid treated multilayer PEDOT:PSS films are stable and of good quality. Both the high transparency and low R_{sq} of these PEDOT:PSS films have showed potential for their use as transparent conductive electrodes in optoelectronic devices.

Acknowledgments: This work was partially supported by the Ministry of Science and Technology (MOST) of Taiwan under contract No MOST 105-2221-E-390-027.

Author Contributions: Po-Wen Sze analyzed the materials; Po-Wen Sze, Kuan-Wei Lee, and Bing-Siang Kao designed the experiments; Po-Wen Sze, Kuan-Wei Lee, Dei-Wei Chou, and Bing-Siang Kao performed the experiments and analyzed the results; Pin-Chiao Huang and Chien-Jung Huang gave some useful information

suggestions for this work and contributed the analysis tools; Po-Wen Sze, Kuan-Wei Lee, and Bing-Siang Kao drafted the manuscript; and Po-Wen Sze and Bing-Siang Kao finalized the manuscript.

Conflicts of Interest: The authors declare no conflict of interest.

References

1. Søndergaard, R.R.; Hösel, M.; Krebs, F.C. Roll-to-roll fabrication of large area functional organic materials. *J. Polym. Sci. Part B Polym. Phys.* **2013**, *51*, 16–34. [[CrossRef](#)]
2. Azzopardi, B.; Emmott, C.J.M.; Urbina, A.; Krebs, F.C.; Mutale, J.; Nelson, J. Economic assessment of solar electricity production from organic-based photovoltaic modules in a domestic environment. *Energy Environ. Sci.* **2011**, *4*, 3741–3753. [[CrossRef](#)]
3. Cui, J.; Wang, A.; Edleman, N.L.; Ni, J.; Lee, P.; Armstrong, N.R.; Marks, T.J. Indium Tin oxide alternatives—High work function transparent conducting oxides as anodes for organic light-emitting diodes. *Adv. Mater.* **2001**, *13*, 1476–1480. [[CrossRef](#)]
4. Park, S.; Tark, S.J.; Kim, D. Effect of sorbitol doping in PEDOT:PSS on the electrical performance of organic photovoltaic devices. *Curr. Appl. Phys.* **2011**, *11*, 1299–1301. [[CrossRef](#)]
5. Shin, D.; Kim, T.; Ahn, B.T.; Han, S.M. Solution-processed Ag nanowires + PEDOT:PSS hybrid electrode for Cu(In,Ga)Se₂ thin-film solar cells. *ACS Appl. Mater. Interfaces* **2015**, *7*, 13557–13563. [[CrossRef](#)] [[PubMed](#)]
6. Zhang, B.; Li, W.; Yang, J.; Fu, Y.; Xie, Z.; Zhang, S.; Wang, L. Performance enhancement of polymer light-emitting diodes by using ultrathin fluorinated polyimide modifying the surface of poly(3,4-ethylene dioxathiophene):poly(styrenesulfonate). *J. Phys. Chem. C* **2009**, *113*, 7898–7903. [[CrossRef](#)]
7. Latessa, G.; Brunetti, F.; Reale, A.; Saggio, G.; Di Carlo, A. Piezoresistive behaviour of flexible PEDOT:PSS based sensors. *Sens. Actuators B Chem.* **2009**, *139*, 304–309. [[CrossRef](#)]
8. Onorato, A.; Invernale, M.A.; Berghorn, I.D.; Pavlik, C.; Sotzing, G.A.; Smith, M.B. Enhanced conductivity in sorbitol-treated PEDOT–PSS. Observation of an in situ cyclodehydration reaction. *Synth. Met.* **2010**, *160*, 2284–2289. [[CrossRef](#)]
9. Ke, J.-C.; Wang, Y.-H.; Chen, K.-L.; Huang, P.-H.; Huang, C.-J. Study of small molecule organic solar cells performance based on boron subphthalocyanine chloride and C₆₀. *Int. J. Photoenergy* **2013**, *2013*, 803126. [[CrossRef](#)]
10. Huang, P.-H.; Huang, C.-J.; Chen, K.-L.; Ke, J.-C.; Wang, Y.-H.; Kang, C.-C. Improved reliability of small molecule organic solar cells by double anode buffer layers. *J. Nanomater.* **2014**, *2014*, 741761. [[CrossRef](#)]
11. Huang, P.-H.; Wang, Y.-H.; Ke, J.-C.; Huang, C.-J. Investigation of various active layers for their performance on organic solar cells. *Materials* **2016**, *9*, 667. [[CrossRef](#)]
12. Havare, A.K.; Can, M.; Demic, S.; Kus, M.; Icli, S. The performance of OLEDs based on sorbitol doped PEDOT:PSS. *Synth. Met.* **2012**, *161*, 2734–2738. [[CrossRef](#)]
13. Nardes, A.M.; Kemerink, M.; de Kok, M.M.; Vinken, E.; Maturova, K.; Janssen, R.A.J. Conductivity, work function, and environmental stability of PEDOT:PSS thin films treated with sorbitol. *Org. Electron.* **2008**, *9*, 727–734. [[CrossRef](#)]
14. Huang, C.-J.; Chen, K.-L.; Tsao, Y.-J.; Chou, D.-W.; Chen, W.-R.; Meen, T.-H. Study of solvent-doped PEDOT:PSS layer on small molecule organic solar cells. *Synth. Met.* **2013**, *164*, 38–41. [[CrossRef](#)]
15. Huang, J.-H.; Kekuda, D.; Chu, C.-W.; Ho, K.-C. Electrochemical characterization of the solvent-enhanced conductivity of poly(3,4-ethylenedioxythiophene) and its application in polymer solar cells. *J. Mater. Chem.* **2009**, *19*, 3704–3712. [[CrossRef](#)]
16. Cruz-Cruz, I.; Reyes-Reyes, M.; Aguilar-Frutis, M.A.; Rodriguez, A.G.; López-Sandoval, R. Study of the effect of DMSO concentration on the thickness of the PSS insulating barrier in PEDOT:PSS thin films. *Synth. Met.* **2010**, *160*, 1501–1506. [[CrossRef](#)]
17. Luo, J.; Billep, D.; Waechtler, T.; Otto, T.; Toader, M.; Gordan, O.; Sheremet, E.; Martin, J.; Hietschold, M.; Zahn, D.R.T.; et al. Enhancement of the thermoelectric properties of PEDOT:PSS thin films by post-treatment. *J. Mater. Chem. A* **2013**, *1*, 7576–7583. [[CrossRef](#)]
18. Kim, M.S.; Park, S.K.; Kim, Y.-H.; Kang, J.W.; Han, J.-I. Glycerol-doped poly(3,4-ethylenedioxythiophene):poly(styrene sulfonate) buffer layer for improved power conversion in organic photovoltaic devices. *J. Electrochem. Soc.* **2009**, *156*, H782–H785. [[CrossRef](#)]

19. Lee, M.-W.; Lee, M.-Y.; Choi, J.-C.; Park, J.-S.; Song, C.-K. Fine patterning of glycerol-doped PEDOT:PSS on hydrophobic PVP dielectric with ink jet for source and drain electrode of OTFTs. *Org. Electron.* **2010**, *11*, 854–859. [[CrossRef](#)]
20. Hu, Z.; Zhang, J.; Hao, Z.; Zhao, Y. Influence of doped PEDOT:PSS on the performance of polymer solar cells. *Sol. Energy Mater. Sol. Cells* **2011**, *95*, 2763–2767. [[CrossRef](#)]
21. Crispin, X.; Jakobsson, F.L.E.; Crispin, A.; Grim, P.C.M.; Andersson, P.; Volodin, A.; van Haesendonck, C.; Van der Auweraer, M.; Salaneck, W.R.; Berggren, M. The origin of the high conductivity of poly(3,4-ethylenedioxythiophene)-poly(styrenesulfonate) (PEDOT-PSS) plastic electrodes. *Chem. Mater.* **2006**, *18*, 4354–4360. [[CrossRef](#)]
22. Yan, H.; Okuzaki, H. Effect of solvent on PEDOT/PSS nanometer-scaled thin films: XPS and STEM/AFM studies. *Synth. Met.* **2009**, *159*, 2225–2228. [[CrossRef](#)]
23. Alemu Mengistie, D.; Wang, P.-C.; Chu, C.-W. Effect of molecular weight of additives on the conductivity of PEDOT:PSS and efficiency for ITO-free organic solar cells. *J. Mater. Chem. A* **2013**, *1*, 9907–9915. [[CrossRef](#)]
24. Yagci, Ö.; Yesilkaya, S.S.; Yüksel, S.A.; Ongül, F.; Varal, N.M.; Kus, M.; Günes, S.; Icelli, O. Effect of boric acid doped PEDOT:PSS layer on the performance of P3HT:PCBM based organic solar cells. *Synth. Met.* **2016**, *212*, 12–18. [[CrossRef](#)]
25. Pettersson, L.A.A.; Ghosh, S.; Inganäs, O. Optical anisotropy in thin films of poly(3,4-ethylenedioxythiophene)-poly(4-styrenesulfonate). *Org. Electron.* **2002**, *3*, 143–148. [[CrossRef](#)]
26. Timpanaro, S.; Kemerink, M.; Touwslager, F.J.; De Kok, M.M.; Schrader, S. Morphology and conductivity of PEDOT/PSS films studied by scanning-tunneling microscopy. *Chem. Phys. Lett.* **2004**, *394*, 339–343. [[CrossRef](#)]
27. Meen, T.-H.; Chen, K.-L.; Chen, Y.-H.; Chen, W.-R.; Chou, D.-W.; Lan, W.-H.; Huang, C.-J. The Effects of dilute sulfuric acid on sheet resistance and transmittance in poly(3,4-ethylenedioxythiophene):poly(styrenesulfonate) films. *Int. J. Photoenergy* **2013**, *2013*, 843410. [[CrossRef](#)]
28. Xia, Y.; Sun, K.; Ouyang, J. Solution-Processed metallic conducting polymer films as transparent electrode of optoelectronic devices. *Adv. Mater.* **2012**, *24*, 2436–2440. [[CrossRef](#)] [[PubMed](#)]
29. Garreau, S.; Duvail, J.L.; Louarn, G. Spectroelectrochemical studies of poly(3,4-ethylenedioxythiophene) in aqueous medium. *Synth. Met.* **2001**, *125*, 325–329. [[CrossRef](#)]
30. Ha, Y.H.; Nikolov, N.; Pollack, S.K.; Mastrangelo, J.; Martin, B.D.; Shashidhar, R. Towards a transparent, highly conductive poly(3,4-ethylenedioxythiophene). *Adv. Funct. Mater.* **2004**, *14*, 615–622. [[CrossRef](#)]
31. Hsiao, Y.-S.; Whang, W.-T.; Chen, C.-P.; Chen, Y.-C. High-conductivity poly(3,4-ethylenedioxythiophene):poly(styrene sulfonate) film for use in ITO-free polymer solar cells. *J. Mater. Chem.* **2008**, *18*, 5948–5955. [[CrossRef](#)]
32. Crispin, X.; Marciniak, S.; Osikowicz, W.; Zotti, G.; van der Gon, A.W.D.; Louwet, F.; Fahlman, M.; Groenendaal, L.; De Schryver, F.; Salaneck, W.R. Conductivity, morphology, interfacial chemistry, and stability of poly(3,4-ethylene dioxythiophene)-poly(styrene sulfonate): A photoelectron spectroscopy study. *J. Polym. Sci. Part B Polym. Phys.* **2003**, *41*, 2561–2583. [[CrossRef](#)]
33. Kim, J.Y.; Jung, J.H.; Lee, D.E.; Joo, J. Enhancement of electrical conductivity of poly(3,4-ethylenedioxythiophene)/poly(4-styrenesulfonate) by a change of solvents. *Synth. Met.* **2002**, *126*, 311–316. [[CrossRef](#)]
34. Xia, Y.; Sun, K.; Ouyang, J. Highly conductive poly(3,4-ethylenedioxythiophene):poly(styrene sulfonate) films treated with an amphiphilic fluoro compound as the transparent electrode of polymer solar cells. *Energy Environ. Sci.* **2012**, *5*, 5325–5332. [[CrossRef](#)]
35. Ouyang, J.; Chu, C.W.; Chen, F.C.; Xu, Q.; Yang, Y. High-conductivity poly(3,4-ethylenedioxythiophene):poly(styrene sulfonate) film and its application in polymer optoelectronic devices. *Adv. Funct. Mater.* **2005**, *15*, 203–208. [[CrossRef](#)]
36. Lang, U.; Müller, E.; Naujoks, N.; Dual, J. Microscopical investigations of PEDOT:PSS thin films. *Adv. Funct. Mater.* **2009**, *19*, 215–220. [[CrossRef](#)]
37. Nardes, A.M.; Kemerink, M.; Janssen, R.A.J.; Bastiaansen, J.A.M.; Kiggen, N.M.M.; Langeveld, B.M.W.; van Breemen, A.J.J.M.; de Kok, M.M. Microscopic understanding of the anisotropic conductivity of PEDOT:PSS thin films. *Adv. Mater.* **2007**, *19*, 1196–1200. [[CrossRef](#)]
38. Zhang, W.; Bi, X.; Zhao, X.; Zhao, Z.; Zhu, J.; Dai, S.; Lu, Y.; Yang, S. Isopropanol-treated PEDOT:PSS as electron transport layer in polymer solar cells. *Org. Electron.* **2014**, *15*, 3445–3451. [[CrossRef](#)]

39. Hansen, W.N.; Hansen, G.J. Standard reference surfaces for work function measurements in air. *Surf. Sci.* **2001**, *481*, 172–184. [[CrossRef](#)]
40. Sommerhalter, C.; Mattes, T.W.; Glatzel, T.; Jäger-Waldau, A.; Lux-Steiner, M.C. High-sensitivity quantitative Kelvin probe microscopy by noncontact ultra-high-vacuum atomic force microscopy. *Appl. Phys. Lett.* **1999**, *75*, 286–288. [[CrossRef](#)]
41. Huang, J.; Miller, P.F.; Wilson, J.S.; deMello, A.J.; deMello, J.C.; Bradley, D.D.C. Investigation of the effects of doping and post-deposition treatments on the conductivity, morphology, and work function of poly(3,4-ethylenedioxythiophene)/poly(styrene sulfonate) films. *Adv. Funct. Mater.* **2005**, *15*, 290–296. [[CrossRef](#)]



© 2017 by the authors. Licensee MDPI, Basel, Switzerland. This article is an open access article distributed under the terms and conditions of the Creative Commons Attribution (CC BY) license (<http://creativecommons.org/licenses/by/4.0/>).